INTERNATIONAL JOURNAL OF INTEGRATED ENGINEERING
ISSN: 2229-838X e-ISSN: 2600-7916

IJIE

Vol. 16 No. 5 (2024) 224-249
https://publisher.uthm.edu.my/ojs/index.php/ijie

Implementation of A Comprehensive Mechanistic Model for The Prediction of Erosive Wear in Pipelines Due to Solid Particles Impact

Martins Obaseki[1], Paul T. Elijah[1], Peter B. Alfred[2], Silas Oseme Okuma[1]*

[1] *Department of Mechanical Engineering, Faculty of Engineering, Nigeria Maritime University, Okerenkoko, NIGERIA*

[2] *Department of Mechanical Engineering, Faculty of Engineering, University of Port Harcourt, Port Harcourt, NIGERIA*

*Corresponding Author: silasoseme@gmail.com
DOI: https://doi.org/10.30880/ijie.2024.16.05.018

Article Info

Received: 18 October 2023
Accepted: 11 June 2024
Available online: 1 August 2024

Keywords

Erosive model, ANSYS fluent, impact angle, particle velocity, eroded crater

Abstract

In this paper, implementation of a comprehensive mechanistic model for the prediction of erosive wear in pipelines due to solid particles impact was investigated. The aim of this study is to develop a mechanistic model coupled with CFD model to predict the rate of inner-wall erosive wear of pipeline due to the presence of solid particles. This mechanistic model was developed based on Hertzian contact, and Du and Wang elastoplastic impact models; taking the deformation of the erodent particles and the effective impact angle into consideration. The developed models were compared with experimental data from three different sources and with built-in erosion models in FLUENT. The outcome of the simulation show that the developed model is 92% accurate when compared with the experimental values. The mechanistic model of this study shows a good agreement with the existing models. The trend of variation of erosive wear rate with impact angle, particle velocity, and mass flow rate was the same for all the tested models and a robust improvement in the newly developed models. Erosion of coal-liquid slurry in pipelines was also studied in FLUENT using the developed model UDF. The results of the study show that coal-liquid slurry causes erosion in both bent and straight pipe. The point of dense erosion was observed to have drifted along the straight pipeline as the velocity increases, which implies that little or no erosion will be observed when a very high velocity slurry flows through a short straight pipe spool. It is expected that the results of this work will be of significant help for the strengthening of the application of mechanistic models for predicting inner-wall erosive wear. This model can be effectively applied in oil and gas industries worldwide for accurate prediction of inner-wall erosive wear.

1. Introduction

Slurry flow in pipelines is one of the common ways of transporting coal from the point of mining to where it is utilized. Slurry flow is a combination of liquid and solid in a single flow in pipelines. Slurry flow is mostly turbulent so as to prevent particle settlings in the pipeline bed when they are been carried along the career fluid in the pipeline. Slurry pipelines are not only for transporting coal but for long distance transportation other mining and chemical products such as iron, copper, phosphate concentrates oil-sand mixture and other mineral ores [1, 2]. In

the petroleum industries, oil and gas taken from wells through pipelines can be described as a form of slurry flow consisting of fluid (oil or gas), sand and several other solid particle components [3, 4].
One of the problems of slurry pipelines is erosive wear which occurs in internal surfaces, bents and fittings. The erosion of the pipelines' internal surface is as a result of repeated particle impact causing several indentations, cuttings, gradual removal and wearing away of the surface [5]. Erosive wear in pipelines cause reduction in the pipe thickness thereby reducing the integrity of the pipe and the ability to withstand high pressures. Also, erosive wear in pipelines create spots where pitting corrosion may likely emanate, especially when the pipeline is temporarily out of service. If erosion is not properly monitored, it can be hazardous and can lead to complete damage and shut down of pipelines and the entire production facilities, leading to economic loss [2, 4].

An in-depth understanding of the mechanism and processes of erosion and the methods of controlling or monitoring them is necessary, especially in oil and gas industries and other chemical industries transporting products through pipelines. Estimating the erosive rate of pipelines is a tedious one; however, researchers in the field of Computational Fluid Dynamics (CFD) are doing more work aimed at simplifying the analysis of erosion rate. One of the ways to do this is mathematical modeling and simulations. A Simple mathematical model is developed, then written in CFD codes and run in a software such as ANSYS which produces the result in a graphical user interface (GUI) for better understanding. There are many existing erosion models, some of which will be look at here.

The erosive wear model of particles flowing in fluid and impinging in a surface was first proposed by Finnie [6]. Finnie developed an erosion model in which the volume of materials removed per impact is proportional to the square of the particle impact velocity and depends on other factors such as impact angle and the particle mass. Bitter [7] and Bitter [8] proposed another model for erosion due to impact. He explained that impact by particle can either cause indentation or scratching of the surface, all depending on the particle impact angle. Bitter's erosion volume rate is the sum of the eroded volume due to indentation and that due to scratching or cutting processes. Bitter's model was later modified for ductile materials by Nelson and Gilchrist [9]. Nelson and Gilchrist [9] erosion model was based on their experimental data and it is a two-part equation model: one-part accounting for deformation and the other part for cutting mechanism. Hashish [10] presented a modified model of Finnie erosive wear model. In the modified model, the impact velocity exponent of Finnie which was originally 2 was changed to 2.5. The impact angle function was also modified. Hashish also introduced the particle shape function in the modified model. Huang et al. [11] developed a model which includes both indentation and cutting of the target material and also accounts for property of both the erodent and the target that aid erosion. The model was compared with experimental data of Bitters and Finnie and good agreement was reported. Huang et al. [11] noted that particle impingement on straight pipe wall is due to gravitational settling and turbulence fluctuation and as such the impact angle is much smaller, however there are much larger impact angle at bents and fittings leading to much erosion in them.

Many empirical correlation models for erosive wear were formulated by researchers most of which are based on experimental data. Most of these correlations are preferable in industrial application and are included in Codes and Standards. Some of these correlation models will be discussed briefly here; The Erosion and Corrosion Research Center (E/CRC) of the University of Tulsa developed an empirical erosive wear model for carbon steel based on direct experimental data McLaury [12]. In this model, some key parameters such as the erodent sharpness factor and the target hardness were considered. Oka et al. [13] developed an empirical model for erosion of material surface due to particle impingement. Many influencing factors which include target material hardness and mechanical properties of the erodent. Oka and Yoshida [14] modified the model in part 2 of their article by including the reference erodent particle velocity and diameter. Oka's model is also applicable for predicting erosive wear in ductile materials. The model was one of the preferable models for predicting erosion. Det Norske Veritas [15] developed an empirical erosive wear model popularly known as the DNV model for predicting erosion in straight, bent pipes and pipe fittings. Large number of experimental data and numerical results were gathered to formulate the model. The DNV erosion model was found to predict erosion rate at better accuracy when compared with experimental data from a different sources other than that of the developer Peng and Cao [16].

Other erosive wear models were also reported by Ahlert, [17], Meng and Ludema, [18], Hutchings, [19], Chen et al. [20] etc. Most of these models are empirical correlation and are material specific, that is, they are developed based on the experimental data obtained from experiment performed on a particular target material and erodent. One major problem with empirical models is that they may fail if used to predict erosion of materials with different properties from the one used in developing it. For instance, Oka's model was more realistic, but it was reported by Peng and Cao, [16] to have deviated in the prediction of erosion rate of steel pipe elbow when compared with experimental data of Eyler, [21]. Only few specific empirical correlation models have been reported for slurry pipelines.

There are researches on the topic, however, reliable mechanistic models for prediction of erosive wear related problems are still needed in this field, hence this study. The intent of this study is to develop a mechanistic model coupled with CFD model to predict the rate of inner-wall erosive wear of pipeline due to the presence of solid

Int. Journal of Integrated Engineering Vol. 16 No. 5 (2024) p. 224-249

particles. The mechanism and processes of erosive wear can be studied with ease by the use of Computational Fluid Dynamics (CFD) simulation software. CFD software such as ANSYS FLUENT has been a great tool for turbulent and laminar fluid flow in channels and pipes. The software has the ability to track the flow part of the individual particles and the angle at which they impinge on the surface of the target material. Models for erosive wear are better verified in CFD software because large varieties of test conditions necessary to verify the accuracy of the model are available. To study the erosion in carbon steel pipelines due to slurry particles impact, this study will attempt to develop a more general and mechanistic model to ascertain inner-wall erosion wear rate. The model will first be validated in ANSYS FLUENT using experimental data, and then get tested against some preferable existing erosive wear models for carbon steel in this study.

2. Materials and Method

The aim of this study is to develop an inner-wall erosive wear rate mechanistic model that can predict erosion of pipeline due to the presence of solid particles. A mechanistic inner-wall erosive wear rate model was developed based on Hertzian contact model and Du and Wang elastoplastic impact model, taking the deformation of the erodent particles and the effective impact angle into consideration. The developed model was compared with experimental data and with other models using ANSYS FLUENT in order to showcase the accuracy and universal applicability of the developed model. It is expected that the outcome of this study will be of significant help for the strengthening of the universal application of mechanistic models for predicting erosion rate.

2.1 Erosion Model

There are several erosion models; however, most of the models are empirical correlations. Most of the existing empirical models are CFD-based erosion models, some of which are already built-in in ANSYS FLUENT. The study will look at different predictive equation models which include Finnie's model, Oka's model, DNV model and the E/CRC erosion model.

The Finnie erosion model was developed by Finnie et al. [22] and is given by Brown as, [23];

$$E_v = CV_p^n g(\alpha) \tag{1a}$$

$$g(\alpha) = \begin{cases} \frac{1}{3}cos^2\alpha & for\ \ 18.5^0 \le \alpha \le 90^0 \\ \sin(2\alpha) - 3sin^2\alpha & for\ \ \alpha \le 18.5^0 \end{cases} \tag{1b}$$

Where; E_v is the erosion rate, C is the target material constant n is the velocity exponent. α is the impact angle.

The Oka's model was proposed from experimental results of Oka and Yoshida, [14] and Oka et al. [13]. The Oka's model is given as;

$$E_v = \left[10^{-9} m_p k (H_v)^{k_1} \left(\frac{V_p}{V'}\right)^{k_2} \left(\frac{d}{d'}\right)^{k_3}\right] g(\alpha) \tag{2a}$$

$$g(\alpha) = (\sin\alpha)^{n_1}[1 + H_v(1 - sin\alpha)]^{n_2} \tag{2b}$$

Where; E_v is the erosion rate $(m^3/impact)$, H_v is the Vickers hardness of the target materials, m_p is the mass of the particle, V' and d' are the reference velocity and diameter of particle. $k, k_1, k_2, k_3, n_1, n_2$ are constants depending on the particle type.

Det Norske Veritas formulated an erosion model in 2007 known as the DNV model [15]. The erosion model was developed based on experimental data. The model predictive equation is given as;

$$E_v = KV_p^n g(\alpha) \tag{3a}$$

$$g(\alpha) = \sum_{i=1}^{8} (-1)^{i+1} A_i \alpha^i \tag{3b}$$

Where; E_v is the erosion rate, K is the target material constant (K =2 x10^{-9} for steel), n is the velocity exponent (n = 2.6 for steel), A_1 *to* A_8 are given in order as; 9.37, 42.295, 110.864, 175.804, 170.137, 98.398, 31.211, and 4.17.

E/CRC Erosion Model was proposed by the Erosion /Corrosion Research Center (E/CRC) of the University of Tulsa McLaury, [12]. The erosion model was developed based on experimental data obtained by direct impact of particles of different shapes on carbon steel. The model is given as reported in Zhang et al. [24] as;

$$E_v = Kf(BH)^{-0.59}V_p^n g(\alpha) \tag{4a}$$

$$g(\alpha) = \sum_{i=1}^{5} A_i \alpha^i \tag{4b}$$

Where; E_v is the erosion rate, K is the target material constant (K =2.17 x10^{-7} for carbon steel), n is the velocity exponent (n = 2.41 for carbon steel), BH is the Brinell hardness of target material, f is the particle sharpness factor ($f = 1$) for sharp angular shape, $f = 0.53$ for semi-round, $f = 0.2$ for fully round shape. A_1 *to* A_5 are given in order as; 5.3983, -10.1068, 10.9327, -6.3283, and 1.4234.

2.2 New Erosion Wear Model Development

Erosion of coal slurry pipeline is due to particles impact on the wall of the pipe. The impacting particles cause elastic-plastic deformation of the surface of the pipeline creating temporary asperity-like-protrusions which are washed away by the combined effect of fine particles and high-pressured flowing fluid.

2.2.1. Impact Velocity and Impact Angle

Particles in a slurry flow always impact on the walls and bent of the pipeline conveying the slurries. Most times, the particles impact on the pipeline at angles called the impact angle. The impact angle depends on the particle trajectory, and as such impacts angle varies depending on the turbulence of the slurry flow.

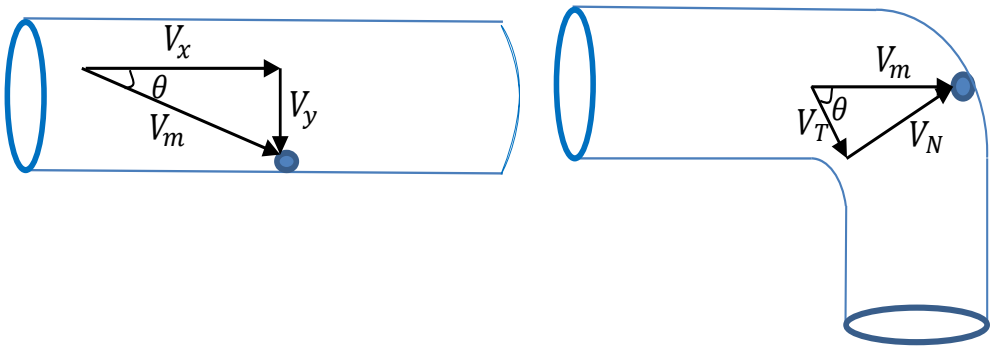

Fig. 1 *Impact velocity and impact angle*

The particle velocity is in the direction of flow, but may swill due to turbulence and hit the adjacent surface at angle. From Fig 1, the vertical component of the velocity V_y is directed. Where; V_x is the horizontal component of the velocity of impact, θ is the impact angle, V_m is the impact velocity, V_N is the velocity normal to the elbow surface and V_T is the tangential velocity of the particle on the elbow surface. From Fig 1, the impact angle and the impact velocity can be calculated as;

$$\theta = \tan^{-1}\left(\frac{V_y}{V_x}\right) = \tan^{-1}\left(\frac{V_N}{V_T}\right) \tag{5}$$

The vertical and the horizontal components of the impact velocity is given in terms of α as;

$$V_x = V_T = V_m \cos\alpha \tag{6a}$$

Int. Journal of Integrated Engineering Vol. 16 No. 5 (2024) p. 224-249

$$V_y = V_N = V_m \sin\alpha \tag{6b}$$

Where; α is a function of θ. For ductile material, the effective value of the impact angle has been modeled by many researchers. In this study, carefully studying the E/CRC model and the DNV model, the impact angle function is proposed as;

$$\alpha = \sum_{i=1}^{5} A_i \theta^i \tag{7a}$$

Where; A_1 *to* A_5 are given in order as; 4.15, -9.62, 11.02, -6.26, and 1.368. Expanding (7a) and inserting the numerical values of A_i gives;

$$\alpha = 4.15\,\theta - 9.62\,\theta^2 + 11.02\,\theta^3 - 6.26\,\theta^4 + 1.368\,\theta^5 \tag{7b}$$

θ is in Radian, therefore, α in this study is computed in Radian and the final result converted to degrees. Fig 2 shows the variation of impact angle function α with θ for DNV, E/CRC and this study.

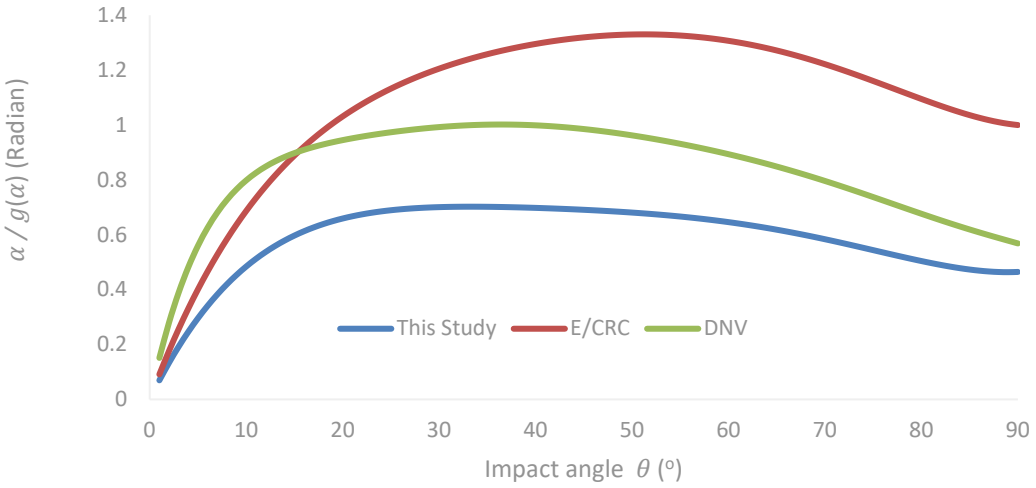

Fig. 2 *Variation of* α *and* $g(\alpha)$ *with* θ

2.2.2. Impact Erosion Damage

According to impact theory, when two bodies collide, they deform. The depth of deformation is a function of yield strength (or Hardness of the bodies). For the case of slurry flow in pipeline, the indenters are the suspended slurry particles and the target is the pipeline. According to Du and Wang [25], the interaction of two bodies during impact can be divided into elastic and elastoplastic region. The impact model is given as;

$$m\ddot{\delta} + F = 0 \tag{8}$$

Where; δ is relative indentation of the impacting bodies (m), F is the impact force (N), $m = m_1 m_2/(m_1 + m_2)$ and m_1, m_2 are the masses of the two impacting bodies. The elastic deformation is model due to Hertz theory and the impact force is given as;

$$F_e = \frac{4}{3} E R^{1/2} \delta^{3/2} \qquad for \quad 0 \le \delta \le \delta_e \tag{9}$$

Where; δ_e is maximum elastic indentation, E and R are the equivalent elastic modulus and radius given as;

$$E = \left[\frac{1 - v_1^2}{E_1} + \frac{1 - v_2^2}{E_2}\right]^{-1} \tag{10}$$

$$R = \left[\frac{1}{r_1} + \frac{1}{r_2}\right]^{-1} \tag{11}$$

Where; E_1 and E_2 are the elastic modulus of the indenter and the target respectively, v_1 and v_2 are the poison ratio for indenter and target respectively and r_1 and r_2 are the radius of indenter and target respectively, for spherical indenter impact on a flat surface target, $R = r_1$. The maximum elastic indentation has been derived for spherical object punch-impact on a flat surface as Du and Wang [25];

$$\delta_e = R\left(\frac{\pi P_0}{2E}\right)^2 \tag{12}$$

Where; P_0 is Maximum impact pressure (Pa). The maximum impact pressure for spherical impactor on a flat surface of the target material at the onset of elastoplastic deformation has been determined to have a value of $P_0 = 2.57\sigma_y$, σ_y is the yield strength of the target material Du and Wang, [25].

The elastic deformation is not permanent, rather it restores to original shape after impact. If the energy of the impactor is enough to go beyond the elastic limit, permanent indentation occurs. For wear to occur in the pipeline, particles impact must cause permanent indentation. Beyond the elastic limit of the target material, plastic indentation occurs in the inner core layers while elastic deformation occurs on the outer layer in contact with the impactor. This is known as elastoplastic deformation. The impact force for elastoplastic deformation has been modeled by Du and Wang [25] for impact of two deformable spheres as;

$$F_{ep} = R\pi P_0\delta - \frac{R^2(\pi P_0)^3}{12E^2} \qquad for \quad \delta_e \le \delta \le \delta_m \tag{13}$$

Where; δ_m is maximum indentation (m). At the end of the impact, the elastic deformation is restituted but the plastic deformation is permanent leaving a crater on the target surface. The relative maximum permanent indentation, δ_p, on the surface due to normal load was derived as Du and Wang, [25];

$$\delta_p = \delta_m - \left[\frac{3R^{1/2}\pi P_0\delta_m}{4E} - \frac{1}{16}\left(\frac{R^{1/2}\pi P_0}{E}\right)^3\right]^{2/3} \tag{14}$$

Equation (13) and (14) was originally developed for impact analysis of two deformable spheres but will be applied here to analyze the deformation of a pipe wall due to spherical particle impact. To apply this model, we assumed that both the impactor and the target are indented, that is; the sum of the indentations of the wall (target), δ_w, and the particle (indenter), δ_s, equals the relative indentation, i.e., $\delta_p = \delta_s + \delta_w$. Also, that the indentation is inversely proportional to Vickers hardness of the materials, i.e, $\delta_s/\delta_w = H_w/H_p$. Where H_p and H_w are the Vickers hardness (GPa) of the solid impacting particles and the pipe wall target respectively. Vickers Hardness, H, in GPa is obtained as, $H\ (GPa) = 0.009807\ H_V$ where H_V is Vickers Hardness Number. Therefore, the non-reversible permanent indentation depth on the pipe wall is given as;

$$\delta_w = \delta_p\left(1 + \frac{H_w}{H_p}\right)^{-1} \tag{15}$$

2.2.3. Erosion Crater Depth

To get the erosion volume per impact, the permanent indentation depth and the crater length are required. From Fig 1, the normal impact velocity, V_y, of particles is due to settling and the tangential impact velocity, V_x, is particle axial velocity.

Int. Journal of Integrated Engineering Vol. 16 No. 5 (2024) p. 224-249

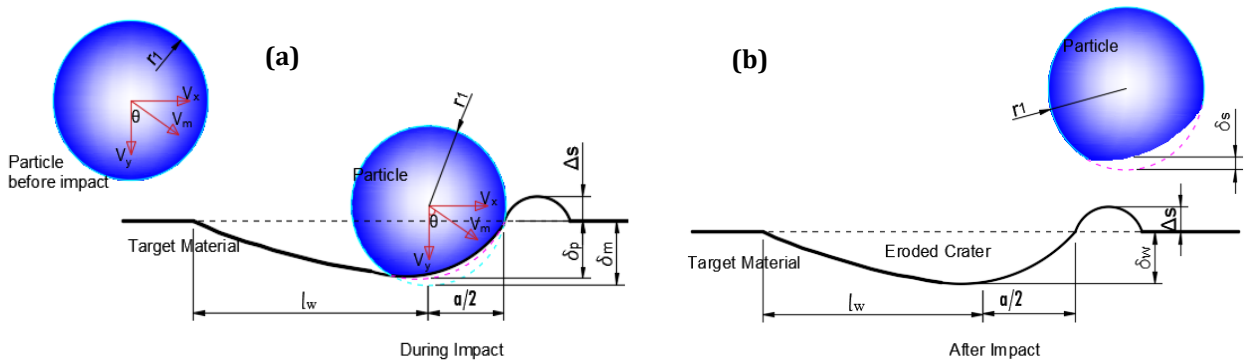

Fig. 3 *Eroded crater due to impact (a) Before impact; (b) After impact*

The study also assumed that the kinetic energy (KE) of particles is completely converted to total work done (W_T) during impact as the indenter decelerates to zero at maximum indentation. Thus, at maximum indentation, the final velocity is zero and the total normal kinetic energy is $KE = \frac{1}{2}mV_m^2Sin^2\alpha$. Where; m = mass of particle.

$$KE = W_T \tag{16}$$

The total Work done, W_T, is the sum of the work done in the elastic, W_e, and elastoplastic, W_{ep}, region during impact.

$$W_T = \int_0^{\delta_e} F_e\, d\delta + \int_{\delta_e}^{\delta_m} F_{ep} d\delta \tag{17}$$

Substituting (9) and (13) into (17) gives the total work done as;

$$W_T = \frac{2}{5}K\delta_e^{5/2} + \frac{1}{2}R\pi P_0\delta_{me}^2 - \frac{R^2(\pi P_0)^3}{12E^2}\delta_{me} \tag{18}$$

Where; $K = \frac{4}{3}ER^{0.5}$ = Hertz constant and $\delta_{me} = \delta_m - \delta_e$

Substituting equation (18) in equation (16) and simplifying gives equation (19) as;

$$\frac{1}{2}R\pi P_0\delta_{me}^2 - \frac{R^2(\pi P_0)^3}{12E^2}\delta_{me} + \frac{2}{5}K\delta_e^{\frac{5}{2}} - \frac{1}{2}mV_m^2Sin^2\alpha = 0 \tag{19}$$

Let;

$$\eta = \frac{R}{6}\left(\frac{\pi P_0}{E}\right)^2 \tag{20a}$$

and

$$\lambda = \frac{4K\delta_e^{5/2}}{5R\pi P_0} - \frac{mV_m^2Sin^2\alpha}{R\pi P_0} \tag{20b}$$

Then, δ_{me} is calculated from equation (19) and (20) as;

$$\delta_{me} = \frac{1}{2}\left(\eta + \sqrt{\eta^2 - 4\lambda}\right) \tag{21a}$$

Equation (21) can be written in terms of the discriminant D_1

$$\delta_{me} = \frac{1}{2}\left(\eta + \sqrt{D_1}\right) \tag{21b}$$

Where; $D_1 = \eta^2 - 4\lambda$. If $D_1 < 0$, then, we set $\delta_{me} = \frac{1}{2}(\eta)$. This is to eliminate chances of getting imaginary solution.

From (21) the maximum relative indentation δ_m is determined as;

$$\delta_m = \delta_{me} + \delta_e \tag{22}$$

Equation (14) and (15) are then used to calculate relative permanent normal depth of indentation, δ_p and permanent normal depth of indentation on the pipe wall δ_w.

2.2.4. Erosion Crater Length

To determine the crater length, δ_l, the average work done to deform a sectional area of depth, $\frac{\delta_m}{2}$, through a length, δ_l, along the target surface was equated to the total tangential kinetic energy of the impacting particle. Assuming no rolling and sliding of particle, the effective eroded crater length is due to the impact force on a smaller average contact area with contact radius $\frac{\delta_m}{4} \leq a$, where a is the maximum contact radius given as; $a = \sqrt{R\delta_m}$. Therefore, going by the equation from Hertz contact model given as; $a = \frac{\pi R P_0}{2E}$ and substituting $a = \frac{\delta_m}{4}$, P_0 is updated as P_t given as;

$$P_t = \frac{\delta_m}{4a} P_0 = 0.25 P_0 \left(\frac{\delta_m}{R}\right)^{1/2} \tag{23}$$

Thus, equation (19) -(22) are updated as;

$$\frac{1}{2} R\pi P_t \delta_{ml}^2 - \frac{R^2(\pi P_t)^3}{12E^2}\delta_{ml} + \frac{2}{5} K\delta_e^{\frac{5}{2}} - \frac{1}{2} m V_m^2 cos^2\alpha = 0 \tag{24}$$

Where; $V_m^2 cos^2\alpha = V_x^2$, $\delta_{ml} = \delta_l - \delta_{el}$, and $\delta_{el} = R\left(\frac{\pi P_t}{2E}\right)^2$

Let;

$$\eta_1 = \frac{R}{6}\left(\frac{\pi P_t}{E}\right)^2 \tag{25a}$$

and

$$\lambda_1 = \frac{4K\delta_e^{\frac{5}{2}}}{5R\pi P_t} - \frac{m V_m^2 cos^2\alpha}{R\pi P_t} \tag{25b}$$

Then, δ_{ml} is calculated from equation (24) and (25) as;

$$\delta_{ml} = \frac{1}{2}\left(\eta_1 + \sqrt{{\eta_1}^2 - 4\lambda_1}\right) \tag{26a}$$

$$\delta_{ml} = \frac{1}{2}\left(\eta + \sqrt{D_2}\right) \tag{26b}$$

Where; $D_2 = {\eta_1}^2 - 4\lambda_1$. If $D_1 < 0$, then, $\delta_{ml} = \frac{1}{2}(\eta_1)$.

From which the maximum relative indentation δ_l is determined as;

$$\delta_l = \delta_{ml} + \delta_{el} \tag{27}$$

$$l_p = \delta_l - \left[\frac{3R^{1/2}\pi P_t \delta_l}{4E} - \frac{1}{16}\left(\frac{R^{1/2}\pi P_t}{E}\right)^3\right]^{2/3} \tag{28}$$

Equation (14) and (15) are updated as (28) and (29) and used to calculate relative permanent eroded crater length, l_p and permanent crater length on the pipe wall, l_w.

Int. Journal of Integrated Engineering Vol. 16 No. 5 (2024) p. 224-249

$$l_w = l_p\left(1+\frac{H_w}{H_p}\right)^{-1} \tag{29}$$

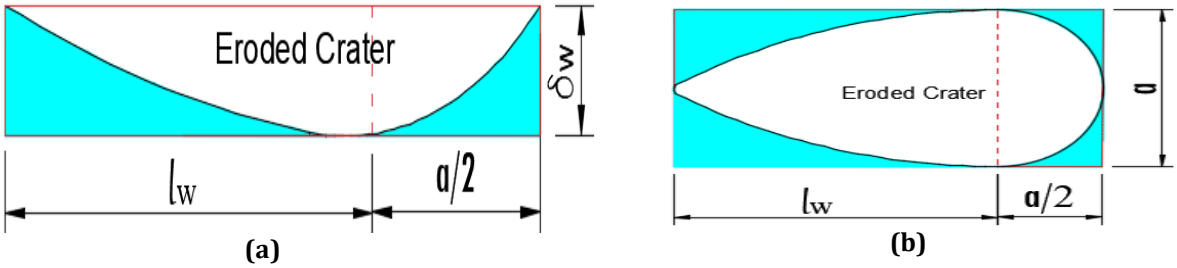

Fig. 4 *Eroded crater due to impact (a) Side view; (b) Top view*

2.2.5 Erosion per Impact

The erosion volume per impact was determined as the one-third of the volume of the cuboid that envelope the eroded crater (fig 4). The length and the depth of the crater were determined from the impact using the Hertzain impact model and the impact model of DU and Wang. The depth of the crater is δ_w, , the width of the crater is $\boldsymbol{a}$ and the length of the crater is (l_w + ½ $\boldsymbol{a}$). One-third of the volume of the cuboid that envelope the crater (which is the erosion volume per impact) is therefore given by equation (30). The Erosion volume, E_v, per impact is calculated from the geometry of the indentation in Fig 4 as;

$$E_v = \frac{1}{3}a\delta_w\left(l_w+\frac{1}{2}a\right) \tag{30}$$

Substituting $a = \sqrt{R\delta_w} = \sqrt{r_1\delta_w}$ and simplifying gives;

$$E_v = \frac{1}{3}\left(l_w r_1^{1/2}\delta_w^{3/2}+\frac{1}{2}r_1\delta_w^2\right) \tag{31}$$

Equation (31) was developed assuming the particles is spherical and that erosion is due to indentation only. To account for cutting effect, the sharpness factor, f, of the particle is incorporated into the equation. Some particles may just slide and roll over the surface of the target causing no indentation, i.e., $E_v = 0$. Some others cause a maximum indentation, i.e., $E_v = E_{v(Max)}$, the erosion of the surface varies from 0, to maximum, so, the average value is taken as; $E_v = \frac{0+E_{v(Max)}}{2}$, Also, a material constant, k, is added to account for target types. k can be calibrated using experimental data. Fig 5 shows the effect of k on the performance of the model. However, for carbon steel material target, we assumed $k = 1$. Therefore, the final erosion volume ($m^3/impact$) is given as;

$$E_v = k\frac{f}{6}\left(l_w r_1^{1/2}\delta_w^{3/2}+\frac{1}{2}r_1\delta_w^2\right) \tag{31}$$

Where; f is the sharpness factor ($f = 1$) for sharp angular shape, $f = 0.53$ for semi-round, and $f = 0.2$ for fully round shape.

The erosion volume in equ.32 can be written as erosion volume per kilogram of particle impact E_v (m^3/kg) divided by particle mass, m. It can also be converted to erosion volume rate, $\dot{E}_v$ (m^3/s), by multiplying it by β, where; $\beta = \frac{\dot{m}}{m}$ is the number of impacting particles per unit time interval, $\dot{m}$ is the mass flow rate of particles and m is the mass of one particle calculated from density and diameter as $m = \frac{\rho\pi d^3}{6}$. $\dot{E}_v$ can also be converted to erosion mass loss rate $\dot{E}_m$ (Kg/s) by multiplying by the target material density, ρ_w. Erosion density, $\dot{E}_d$ (Kg/m^2s), is calculated by dividing $\dot{E}_m$ by the target area, A_t. For $A_t = 1.0\ m^2$, $\dot{E}_d$ (Kg/m^2s) = $\dot{E}_m$ (Kg/s). $\dot{E}_v$ (m^3/s), $\dot{E}_m$ (Kg/s) and $\dot{E}_d$ (Kg/m^2s) are given in equation (33a-c).

$$\dot{E}_v = \beta E_v \tag{33a}$$

$$\dot{E}_m = \beta \rho_w E_v \tag{33b}$$

$$\dot{E}_d = \frac{\beta \rho_w}{A_t} E_v \tag{33c}$$

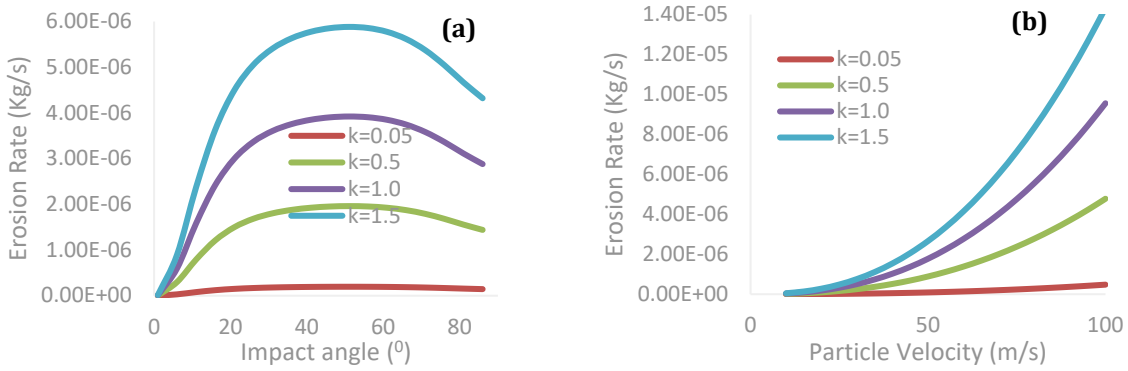

Fig. 5 *Effect of material constant on the developed model (a) Variation with impact angle; (b) Variation with velocity*

3. Results and Discussion

3.1 Implementation of The New Erosion Model in Ansys Fluent

A User-Defined Functions (UDF) of the developed erosion model of this work was written using C++ codes. FLUENT Macros required for the implementation of the UDF were appropriately coded. The UDF were then compiled, built, loaded and hooked with ANSYS FLUENT. Then the erosion rate was simulated and the results obtained were compared with experimental data. Fig 6 shows the flow chart for UDF of the developed model.

Int. Journal of Integrated Engineering Vol. 16 No. 5 (2024) p. 224-249

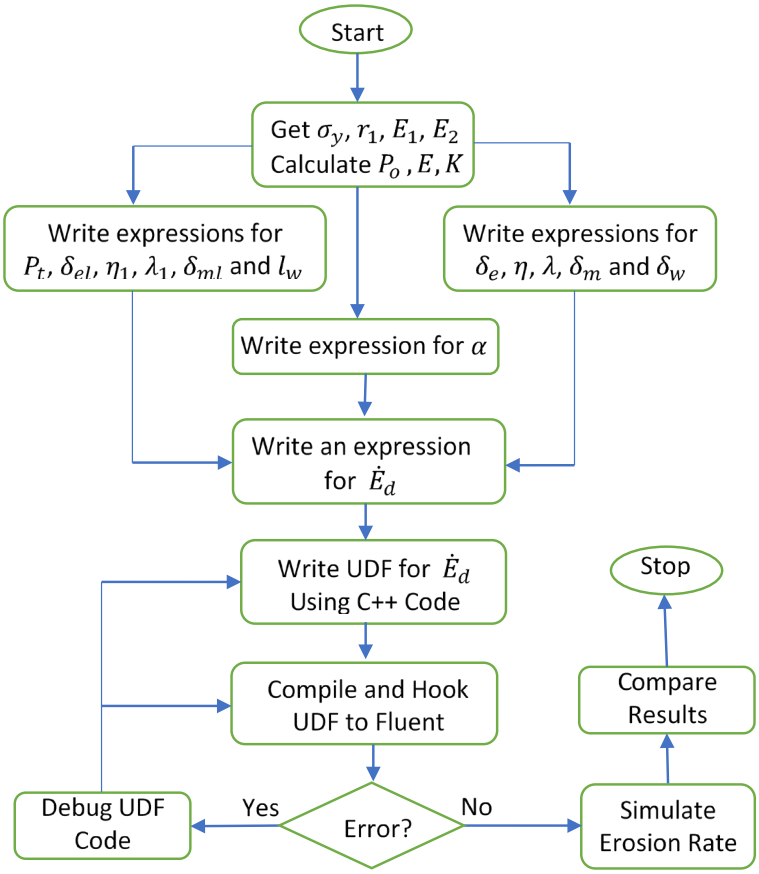

Fig. 6 *Flow chart showing UDF development*

3.2 Model Validation with Experimental Data

Experimental data of [26-29] were employed in this study to further validate the performance of the developed erosion model. Also, the result of the developed model was compared to built-in models in ANSYS 2021 R2 which are Oka, DNV, McLaury and Finnie models. The data for the simulation are given in Table 1. The experimental data are presented in Table 2. The target surface Vickers hardness H_w (GPa) is calculated by using a chart to find the Vickers hardness number equivalent of the Brinell hardness number and multiplying the resultant Vickers hardness number by 0.009807.

Table 1 *Mechanical properties of erodent and target material*

S/N	Target (Steel)		Erodent (S_iO_2)	
	Property	Value	Property	Value
1	H_w	1.24 -1.34 GPa	H_p	20 GPa
2	E_2	209 GPa	E_1	74.8GPa
3	v_2	0.3	v_1	0.17
4	σ_y	250MPa	V	1.0 -300m/s
5	ρ_2	7850 Kg/m^3	ρ_1	2600Kg/m^3

Table 2 *Experimental data used in validating the study model*

Source	Exp No.	Fluid	Diameter	R/D	V(m/s)	d_p(um)	BH	m_p (Kg/s)
Eyler(1987)	A1	Air	41	3.25	25.24	100	120	0.0286
Bourgoyne (1989)	B1-B30	Air	52.5	1.5	47-222	350	120	0.05009 - 0.7473
Bikbaev et al.(1973)	C1-C4	Air	50	2.4 3.6 4.2 7.8	50	295	120	0.3366

Pyboyina (2006)	D1-D3	Air	50.8	1.5	12.2 18.9 28.	150	160	0.00017 0.000521 0.000917

3.3 Geometry and Mesh

The geometry of each of the pipe sizes in Table 2 was modeled in SOLIDWORKS 2021. The same software was used to extract the fluid volume of the pipes and exported to ANSYS 2021 R2. The ANSYS Design Modeler was used to edit the geometry and saved as fluid. Fig 7 shows the fluid volume of the pipe extracted in SOLIDWORKS. Meshing was done in two parts: the surface and the body, using the multi-zone programmed controlled method. The surface meshing was achieved by carefully dividing the edges such that each mesh grid surface area is approximately 1.0 mm^2. The boundary layers were achieved by carefully adjusting the inflation tools. Hexahedral mesh was applied in the entire volume of the fluid. Fig 8 shows the mesh used in the simulation.

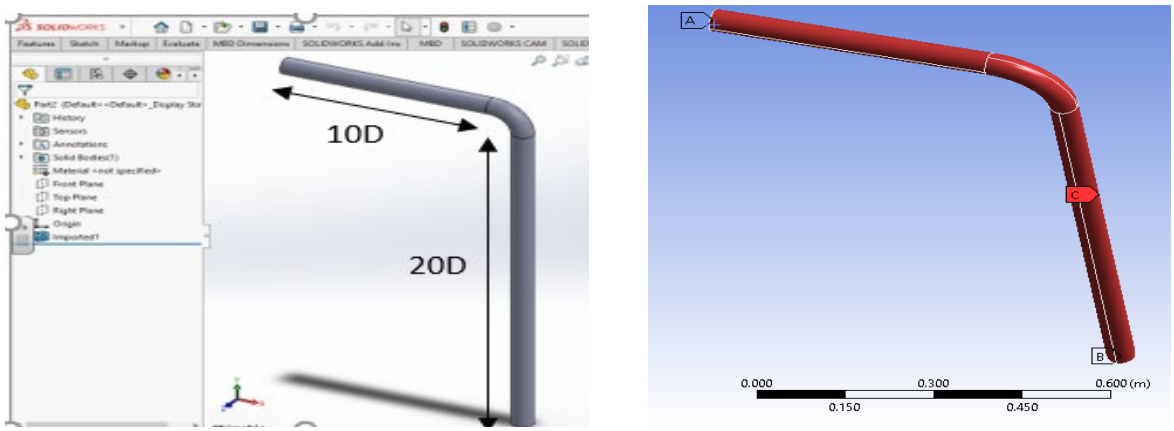

(a) **(b)**

Fig. 7 *Pipe volume geometry (a) Fluid volume exported to Ansys Fluent D = Diameter; (b) Fluid volume ready for mesh generation with name selection viz: A-outlet, B-inlet and C-wall*

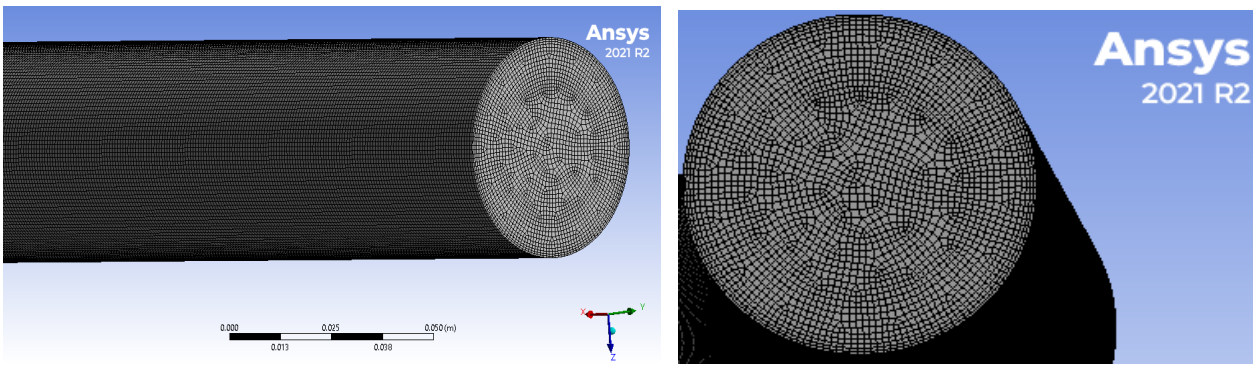

(a) **(b)**

Fig. 8 *Mesh used in the simulation (a) Inlet and wall section; (b) Outlet section*

3.4 Simulation Results Verification

The UDF of the developed model was loaded and hooked into ANSYS FLUENT. The erosion rate was calculated for each of the pipes' data set given in Table 2. The experimental values were originally given as penetration rate in m/s. Multiplying the penetration rate by the density of the eroded surface of steel (7800 kg/m^3) gives the erosion rate in kg/m^2/s. The simulation results were displayed in Table 3. The deviation percentage, Ω (%) defined in (48) was used to compare the deviation of the simulation from the experimental result.

Int. Journal of Integrated Engineering Vol. 16 No. 5 (2024) p. 224-249

$$\Omega(\%) = \frac{Experiment - Predicted}{Experiment} \times 100\% \quad (34)$$

Table 3 *Simulation results compared with experiment*

Source	Exp. Tag.	Exp. No.	Diameter	R/D	V(m/s)	m_p (kg/s)	Exp. (kg/m^2/s)	This Work (kg/m^2/s)	Ω (%)
Eyler (1987)	A1	1	41	3.25	25.24	0.0286	0.000223	0.00112	-66.71
	B2	2	52.5	1.5	72	0.1182	0.01287	0.02164	-25.41
	B3	3	52.5	1.5	93	0.1306	0.02886	0.03738	-12.86
	B5	4	52.5	1.5	98	0.13939	0.038532	0.05651	-18.91
	B6	5	52.5	1.5	103	0.14098	0.041262	0.05287	-12.33
	B8	6	52.5	1.5	169	0.25016	0.37206	0.30317	10.20
	B9	7	52.5	1.5	177	0.3498	0.64974	0.43706	19.57
	B10	8	52.5	1.5	177	0.2915	0.57564	0.39391	18.74
	B11	9	52.5	1.5	178	0.2889	0.50856	0.38415	13.94
	B12	10	52.5	1.5	203	0.2968	0.60528	0.52081	7.50
	B14	11	52.5	1.5	222	0.3021	0.54678	0.65109	-8.71
	B15	12	52.5	1.5	108	0.05009	0.027768	0.02374	7.81
Bourgoye (1989)	B16	13	52.5	1.5	109	0.09249	0.043992	0.03828	6.94
	B17	14	52.5	1.5	108	0.096195	0.041262	0.04182	-0.67
	B18	15	52.5	1.5	104	0.15317	0.077064	0.05651	15.39
	B19	16	52.5	1.5	108	0.17119	0.10764	0.0781	15.91
	B20	17	52.5	1.5	108	0.20776	0.10686	0.08592	10.86
	B21	18	52.5	1.5	107	0.2968	0.11154	0.11381	-1.01
	B22	19	52.5	1.5	111	0.38425	0.20436	0.16095	11.88
	B23	20	52.5	1.5	107	0.60155	0.27768	0.22104	11.36
	B24	21	52.5	1.5	106	0.636	0.25428	0.26959	-2.92
	B25	22	52.5	1.5	103	0.7473	0.23088	0.24726	-3.43
	B27	23	52.5	1.5	100	0.186	0.0624	0.07947	-12.03
	B28	24	52.5	1.5	100	0.305	0.1014	0.10896	-3.59
	B29	25	52.5	1.5	100	0.636	0.2223	0.23599	-2.99
	B30	26	52.5	1.5	100	0.768	0.2184	0.23001	-2.59
Bikbaev et al.(1973)	C2	27	50	3.6	50	0.3366	0.030966	0.02201	16.90
	C3	28	50	4.2	50	0.3366	0.025584	0.02043	11.21
	C4	29	50	7.8	50	0.3366	0.018876	0.01831	1.53
Pyboyina (2006)	D1	30	50.8	1.5	12.2	0.00017	1.59E-07	4.1E-07	-44.02
	D2	31	50.8	1.5	18.9	0.00051	1.42E-06	4.3E-06	-50.41

Fig 9 shows that the developed model results have a good correlation with the experimental results with an R^2 value of 0.9207. It can be concluded from Fig 9(a) that the developed model has 92.07% accuracy. Fig 9(b) shows that the developed model compares well with the experimental.

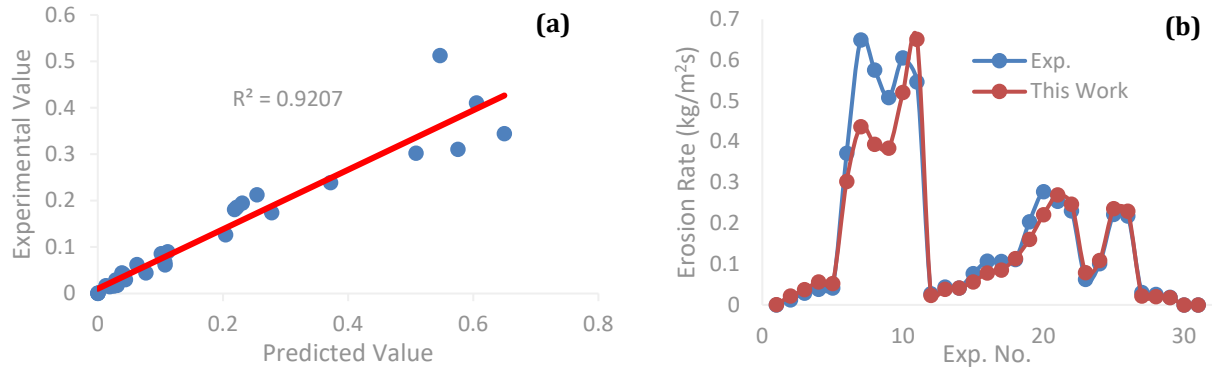

Fig. 9 *Comparing the study model with experimental results (a) Experimental results against predicted results; (b) Experimental results and predicted result against experiment number*

The new erosive wear model in this study was developed by applying the Hertzian impact model and the impact model of Du and Wang. The new model determined erosion of inner-wall of pipeline carrying particle-fluid mixture as function of continuous multiple particles impact on the wall. The calculation procedure is aimed at calculating the volume and weight of materials removed by the individual particles. To achieve this, the impact crater depth and length are computed by the application of existing impact theory. The inner-wall mass loss rate of the target surface is determined by simple dimensional computations which involves the inclusion of the target material density and particles mass flow rate. To better appreciate the developed erosion model of this study; the results were compared to that predicted by Fluent built-in models: Oka, DNV, McLaury and Finnie models. Plotting deviation percentage against velocity for A1-B14 experiments gives the plot in Fig 10(a). Fig 10(a) shows that the model has minimal negative deviation from experimental results due to over-prediction than the other models other than DNV, and has minimal positive deviation due to under-prediction than the DNV. Thus, it is more trusted than the other models. Fig 10(b) compares the built-in models with study model. The study model has better agreement with experimental results than the other models. This is because at 0-5, 12-20 and 25-30 experimental point is more close than other models with the presence of particle diameter as a parameter that have major influence on the results of the study model. Fig 11 is the Fluent simulation output for experimental data B2. The developed model simulation output in Fig 11(e) shows that a wider area on the elbow was deeply eroded, a trend different but is more realistic than the other models.

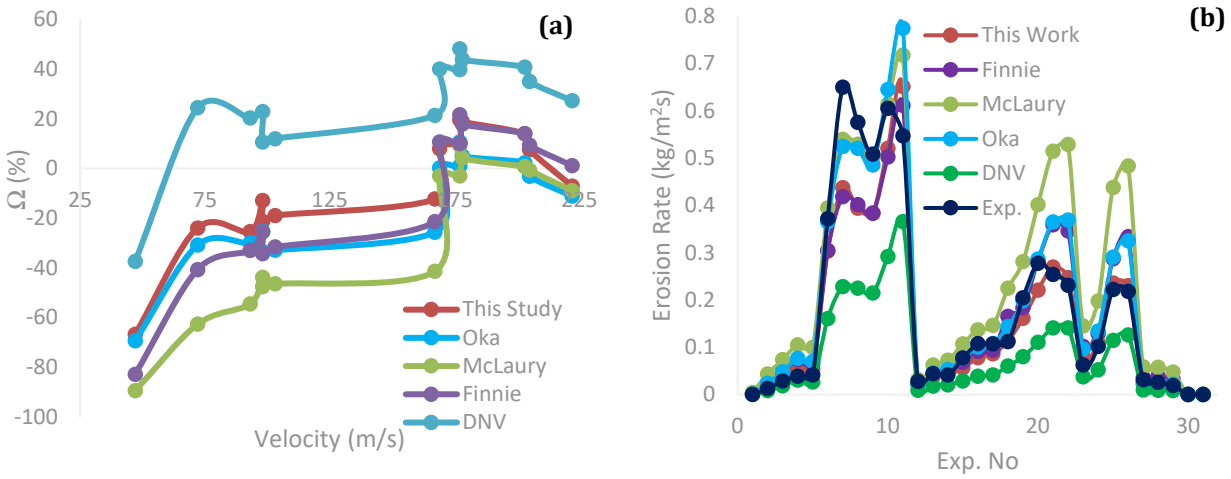

Fig. 10 *Comparing the study model with built-in models; (a) Graph of % error against velocity (A1-B14 data); (b) Graph of erosion rate against experiment number*

Int. Journal of Integrated Engineering Vol. 16 No. 5 (2024) p. 224-249

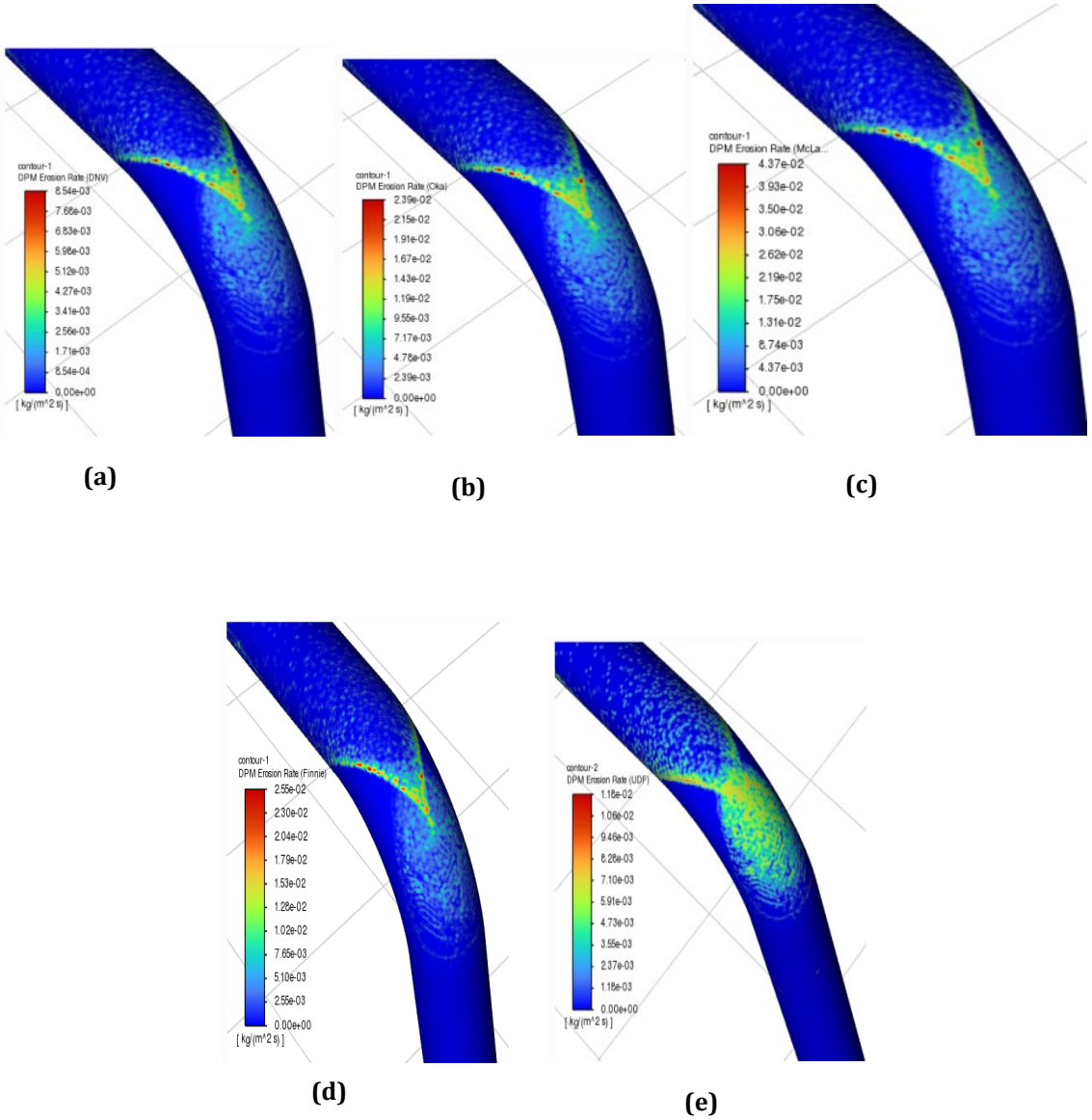

Fig. 11 *Erosion scar on pipe bend (Fluent Output of B2 data); (a) DNV (b) Oka; (c) McLaury; (d) Finnie; (e) The study model*

3.5 Variation with Mass Flow Rate

Experiment B27-B30 has varied mass flow rate at constant velocity of 100m/s and all other parameters are constants. Therefore, B27-B30 was used to study the effect of mass flow rate and the responses of the study model together with the built-in models in Ansys 2021 R2. The study model was found to predict much closer to experimental values than the rest of the models as shown in Fig 12.

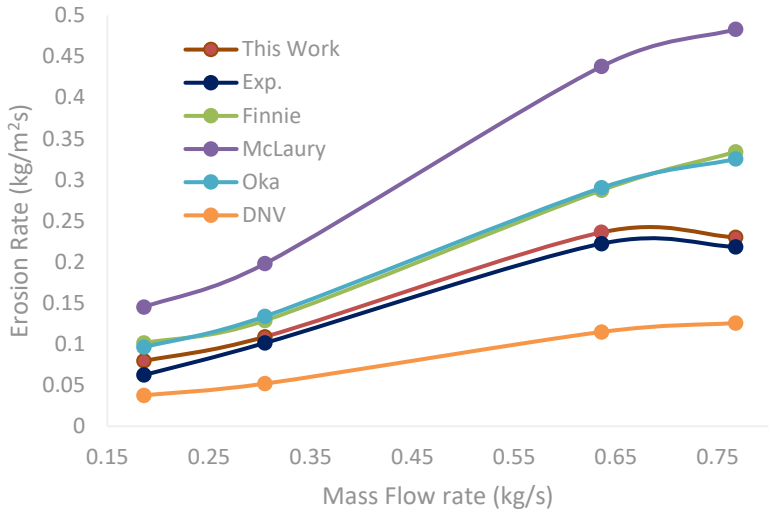

Fig. 12 *Effect of mass flow rate - Comparing the study model with experimental results for B27-B30 data*

3.6 Effect of Bent Radius (R) on Erosive Wear

C2-C4 data has varying R/D ratio and all other parameters are constant. Therefore, the data were used to investigate the influence of bent radius on erosion. R is the radius of pipe bent and D is the diameter of the pipe. For a pipe of fixed diameter as the case of C2-C4, the ratio R/D is a function of bent radius, therefore, increase in R/D ratio translates to increase in bent radius (R). Fig 13 shows that the erosion rate decreases slightly as the R/D increases. The study model shows good agreement with experimental data. Fig 14 shows the simulation output diagram for C4 data. The simulation output of the study model as shown in Fig 14 (e) is more realistic as wider area on two points of the elbow were eroded and the erosion scar spread all over the elbow.

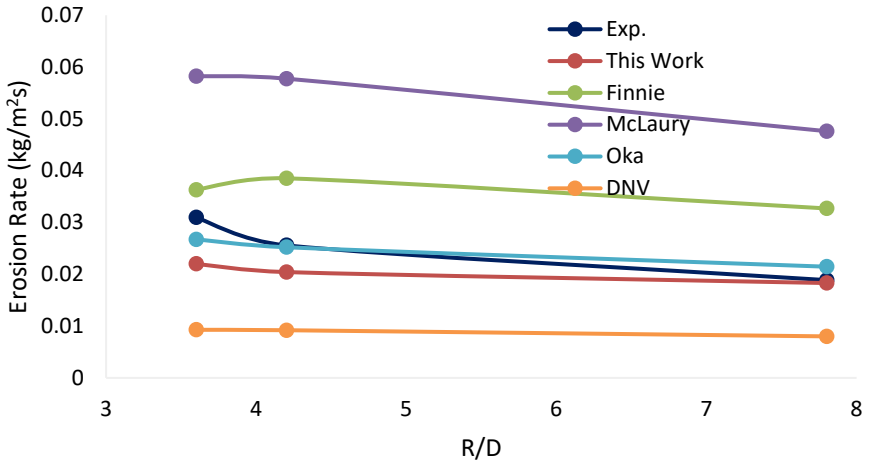

Fig. 13 *Effect of R/D ratio - Comparing the study model with experimental results; C2-C4 data*

Int. Journal of Integrated Engineering Vol. 16 No. 5 (2024) p. 224-249

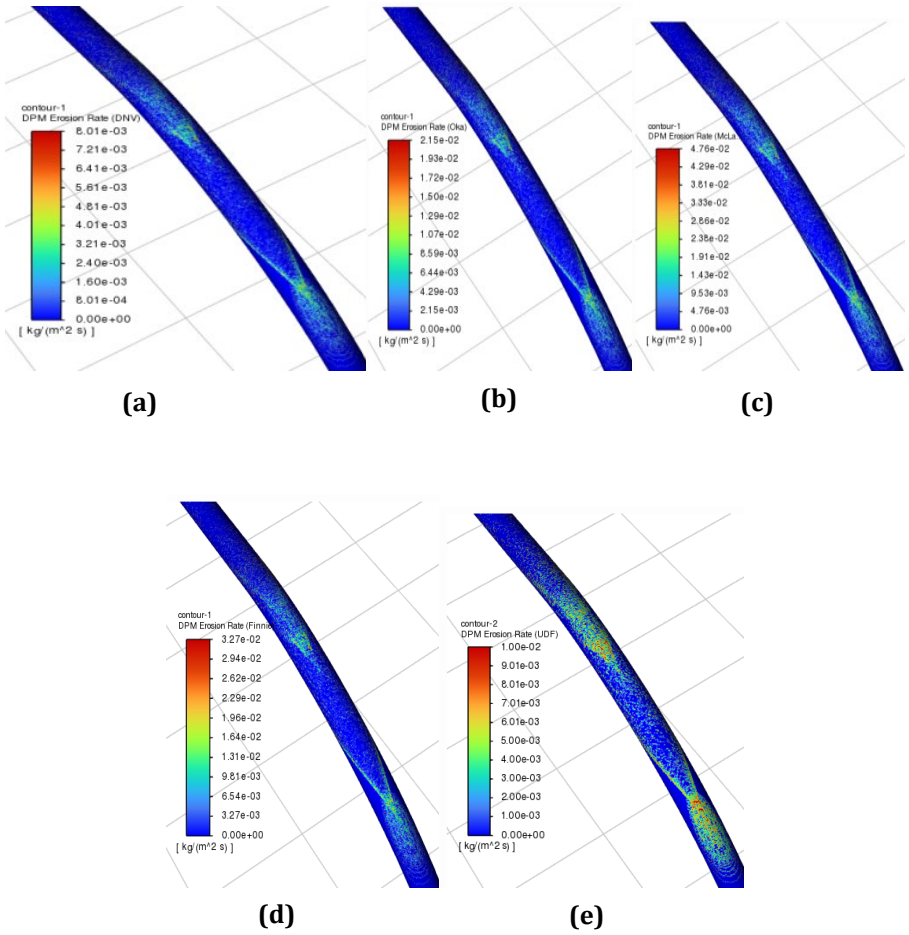

Fig. 14 *Erosion scar on pipe bent (Fluent Output of C4 data);(a) DNV; (b) Oka; (c) McLaury; (d) Finnie; (e) The study Model (UDF)*

3.7. Further Comparison with Other Models

Further validation of the applied model of this study was carried out by direct computation in MATLAB using the Oka's model, DNV model and the E/CRC erosion model. The models' constants are given in Table 4. The erosion rate is calculated in kg/s. Carbon steel target and spherical sand particles (S_iO_2) are considered as erodent. The mechanical properties of the target and the erodent are given in Table 1. The material constant for the developed model was taken as unity for carbon steel material (*k=1*).

Table 4 *Models' constants*

S/N	Oka's Model Constant	Value	DNV Model Constant	Value	E/CRC Model Constant	Value
1	k	65	K	2 x10^{-9}	K	2.17 x10^{-7}
2	k_1	-0.12	n	2.6	N	2.41
3	k_2	$2.3H_w^{0.038}$	A_1	9.37	f	0.2
4	k_3	0.19	A_2	42.295	A_1	5.3983
5	n_1	$0.71H_w^{0.14}$	A_3	110.864	A_2	-10.1068
6	n_2	$2.4H_w^{-0.19}$	A_4	175.804	A_3	10.9327
7	V'	104 m/s	A_5	170.137	A_4	-6.3283
8	D'	326 μm	A_6	98.398	A_5	1.4234
9	a	$0 \leq aH_w \leq 1$	A_7	31.211		
10	b	1	A_8	4.17		

3.7.1. Variation with Impact Angle

The developed mechanistic model in this study was compared to three existing models by direct simulation in MATLAB. The developed model varies with impact angle just like the rest of the models. The developed model agrees more with the DNV and Oka's model at higher velocities. Fig 15 shows the variation of the mechanistic model with the impact angle for a range of 1-90^0. Fig 15 (b) shows an agreement between the proposed model and the DNV model between 0^0 to 90^0 for impact velocity of 300m/s and particles mass flow rate of 0.05kg/s. For a very low impact velocity, there is generally no agreement between the DNV, E/CRC and the developed model of this study as well as the Oka's model. Fig 15 also shows that Oka's models tend to be predicting values higher than the rest. The behaviour is more pronounced at lower velocities as shown in Fig 15 (c) and (d).

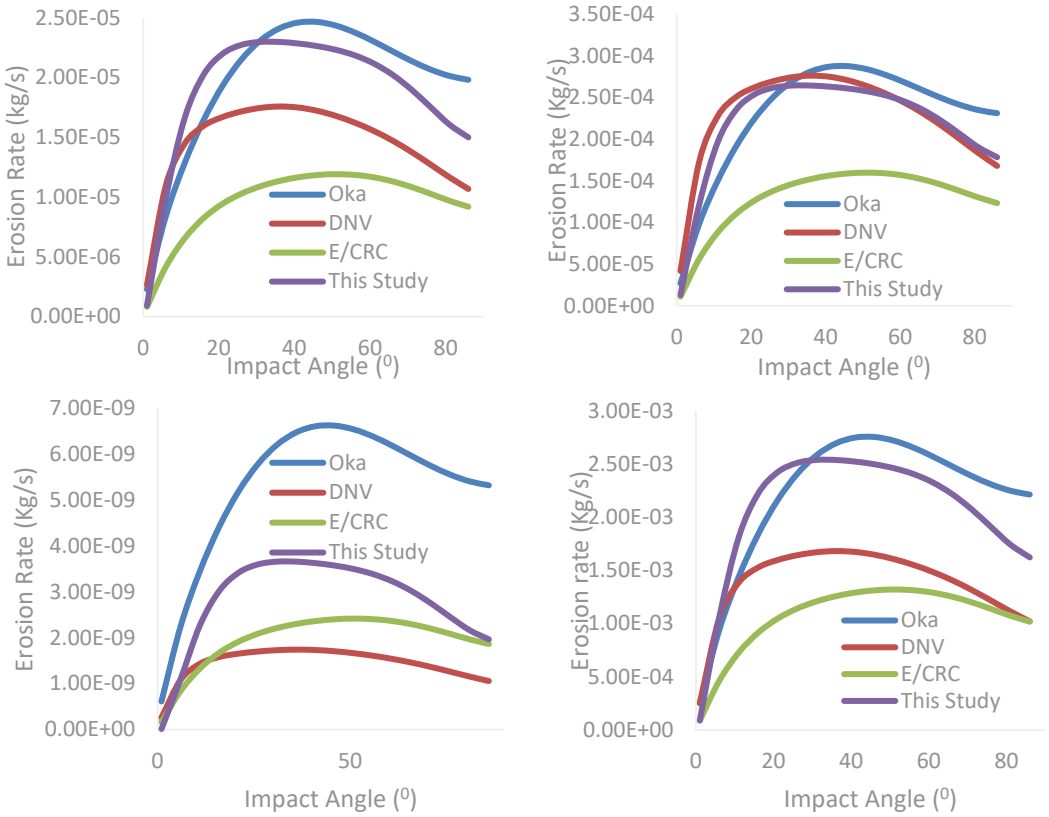

Fig.15 *Effect of impact angle for particle diameter, d = 100 µm*

3.7.2. Variation with Impact Velocity

The effect of impact velocity on the developed model was also investigated in comparison with the selected three models by direct computation in MATLAB. Fig 16 shows that all the four models follow the same trend. The developed mechanistic model competes favorably with the DNV and the Oka's model. Fig 16 (a) and (b) shows that the developed model, DNV and the Oka's model have perfect agree at the different particle mass flow rate. An increase in velocity increases the erosive wear rate because the particle has more kinetic energy which is converted to do more work on the target material causing more wear damage on the material. Higher velocity also means higher turbulence which causes the particle to impact at different angle causing a combine effect of indentation, crack and abrasion, which eventually lead to higher erosive wear.

Fig 16 (a) and (b) shows the effect of particle velocity at higher particle mass flow rate. The model developed in this study show good agreement with the rest of the models at all tested particle velocities. Generally, the developed model is responsive probably because of the inclusion of many materials' mechanical properties in the model. Fig 16 also shows that E/CRC model predicts values that are lower than the rest of the model at all velocities.

Int. Journal of Integrated Engineering Vol. 16 No. 5 (2024) p. 224-249

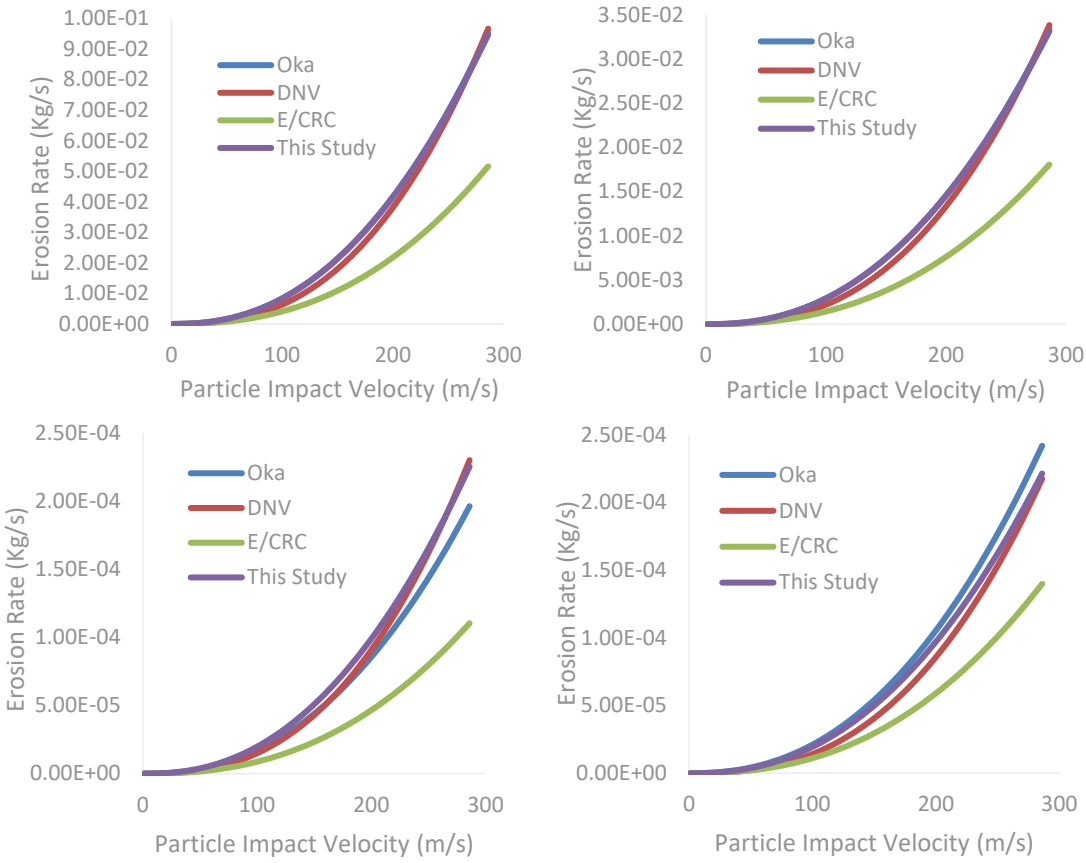

Fig.16 *Effect of impact velocity for particle diameter, d = 100 µm*

3.7.3 Effect of Particle Mass Flow Rate

The effect of mass flow rate of particles on the erosive wear of steel surface and the response of the model developed in this work was also investigated. Fig 17 shows similar trend for all the models. Increase in mass flow rate of particles has a linear effect on the erosive wear rate of the target material. However, the effect of particle mass flow rate is more on the Oka's model than the rest of the models. The developed model of this study shows consistent high response to mass flow rate. However, a much higher agreement is observed between the developed model, DNV and Oka's models for all tested impact angles.

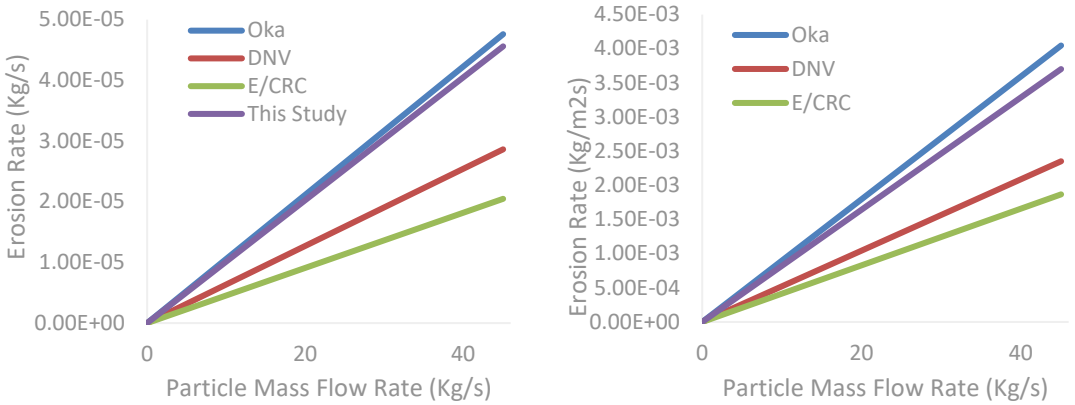

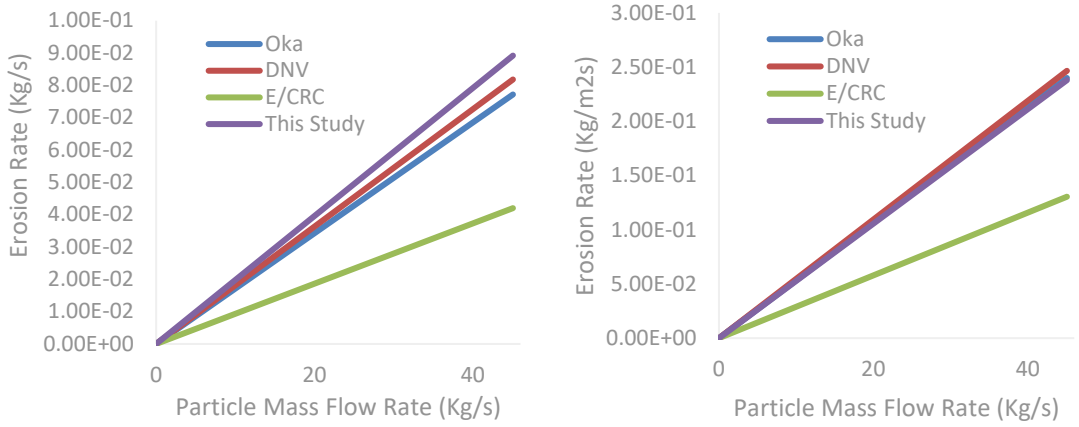

Fig.17 *Effect of particle mass flow rate for particle diameter, d = 100 µm*

3.7.4 Effect of Particle Diameter

The effect of particle diameter is not captured in the empirical correlation of DNV and E/CRC models; however, Oka's correlation model includes the particles average diameter. The developed model, being mechanistic, combines all the material parameters including the particle mean diameter. Fig 18 shows the variation of eroded mass loss with particle diameter.

This study undertakes extra steps to analyze the effect of particle diameter on the erosion rate by plotting eroded mass (kg/Impact) against particle diameter as shown in Fig 18. The result shows that an increase in particle size (diameter) leads to a corresponding increase in indentation or erosive damage for both Oka's and the developed model. The model of DNV and E/CRC did not consider particle diameter as a parameter that have major influence on the results of their models. Theoretically, few larger particles may produce the same effect as the many smaller particles, however, experimental investigations in recent times show slight increase in erosive wear rate as the mean particle sizes increase. From Fig 18 (a) and (b) it can be inferred that larger particles have greater momentum and kinetic energy and as such can cause erosive damage more easily than smaller particles.

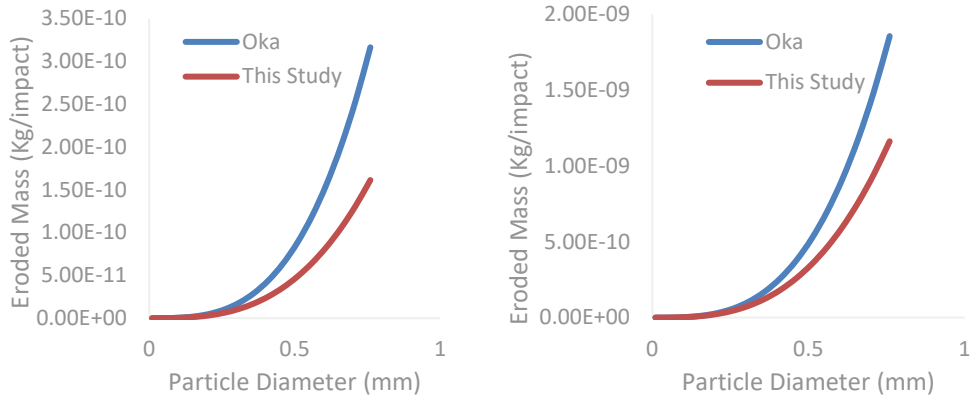

Fig. 18 *Effect of particle diameter on erosive impact damage*

3.7.5 Effect of Elastic Modulus and Yield Strength

The developed model incorporates many mechanical properties of both the target material and the erodent. The effect of the modulus of elasticity and the yield strength of the target material was investigated using the developed model; the results are displayed in Fig 19(a) and Fig 19(b). Fig 19 (a) and (b) show that erosion rate increase with increase in the modulus of elasticity of the target material. The same trend is observed in the equivalent elastic modulus as shown in Fig 11 (b). Fig 20 shows that the erosion rate decreases with increase in the value of the target material yield strength. For Carbon steel, the yield strength is proportional to hardness; therefore, similar trend is expected for material hardness.

Int. Journal of Integrated Engineering Vol. 16 No. 5 (2024) p. 224-249

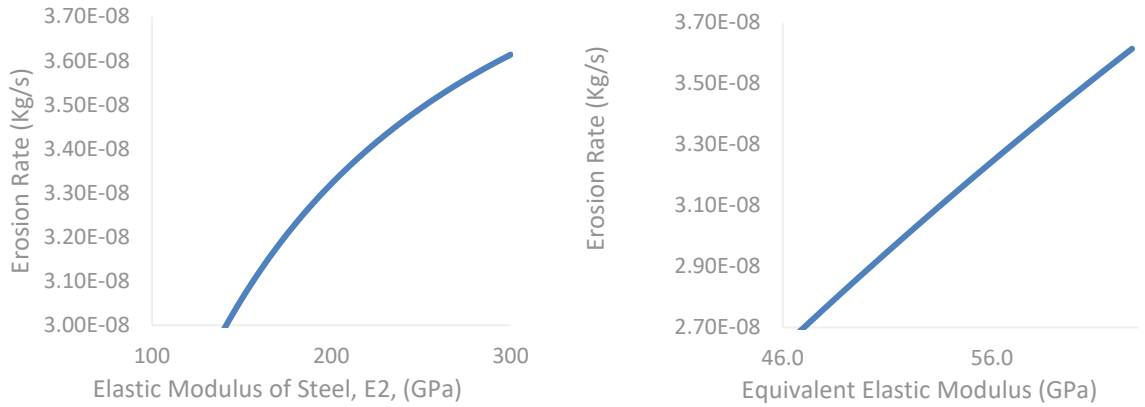

Fig. 19 *Effect of elastic modulus (A) Target material; (B) Equivalent elastic modulus*

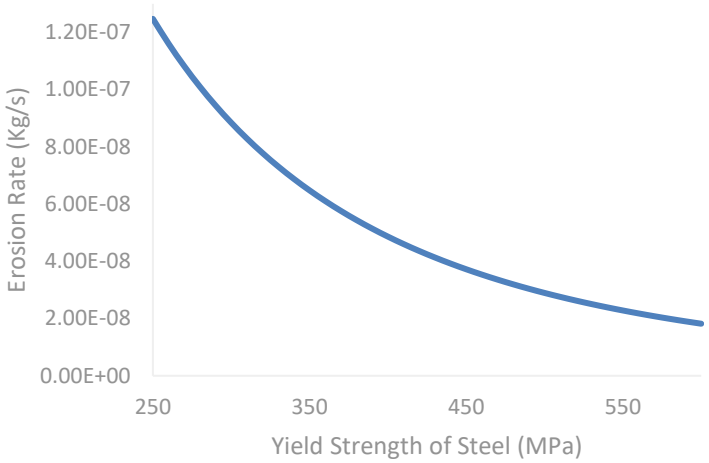

Fig. 20 *Effect of yield strength and hardness*

3.8 Investigation of Erosion in Coal-liquid Slurry Pipeline

The hardness of coal is less than that of steel, however, coal slurries in pipe will still lead to wall thinning of the pipeline due to erosion. To the best of our knowledge, data used in developing most of the empirical erosion models were obtained by using the harder particles as erodent, and softer materials as the target. The existing models, therefore, do not account for the effect of the erodent's hardness and other mechanical properties, thus, may not be accurate in predicting the erosion of steel (harder target) pipeline due to coal (softer erodent) slurry flow. The study model validated in this study offers to be reliable as it accounts for the properties of both erodent and target materials. Therefore, the developed erosion model, haven been validated with experimental data and found to have high accuracy was used in the investigation of erosion rate of coal-liquid slurry pipelines. To investigate the erosion of coal slurry pipelines, anthracite coal with density of 1550 kg/m^3 was used as the erodent materials. The mechanical properties of coal were obtained from [30] as follows; poison ratio = 0.36 and Elastic modulus = 1.56GPa. The yield strength of anthracite coal was obtained from Wang et al. [31] as 88.79 MPa for a small coal particle size. Therefore, a value of 88.79 MPa for 100μm diameter was used in this study. The hardness is calculated from the yield strength as Hp = yield strength (GPa) x 2.8 = 0.25. The carrier fluid is liquid water.

3.8.1 Pipe Elbow

To investigate the erosion of steel pipeline elbow due to coal slurry flow, a vertical pipe elbow of diameter (D) 25mm and R/D ratio of 1.5 was used. The velocity was varied from 12.5m/s to 50m/s and the mass flow rate varied from 0.05kg/s to 5.0kg/s. Fig 21 shows the effect of velocity and mass flow rate on erosion rate. Increase in velocity results in nonlinear increase in erosion rate, while increase in mass flow rate leads to corresponding linear increase in erosion rate. Fig 22 shows that at low velocity as in Fig 22(a), the erosion scar concentrated on the elbow and the V-shaped erosion scar was not found. It shows that the moving particles dissipated most of its energy on the elbow surface and was left with little energy which is incapable of causing further erosion. As the

velocity increases, the V-scar can be seen as shown in Fig 22 (b-e) and minor erosion scars scattered all over the elbow and beyond.

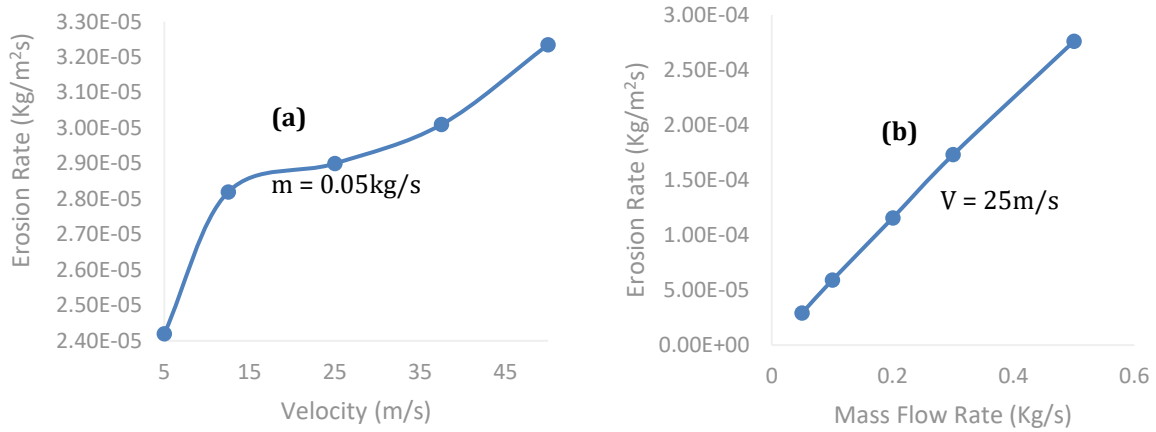

Fig. 21 *Erosion rate of 25mm diameter elbow effect of velocity (b) effect of mass flow rate*

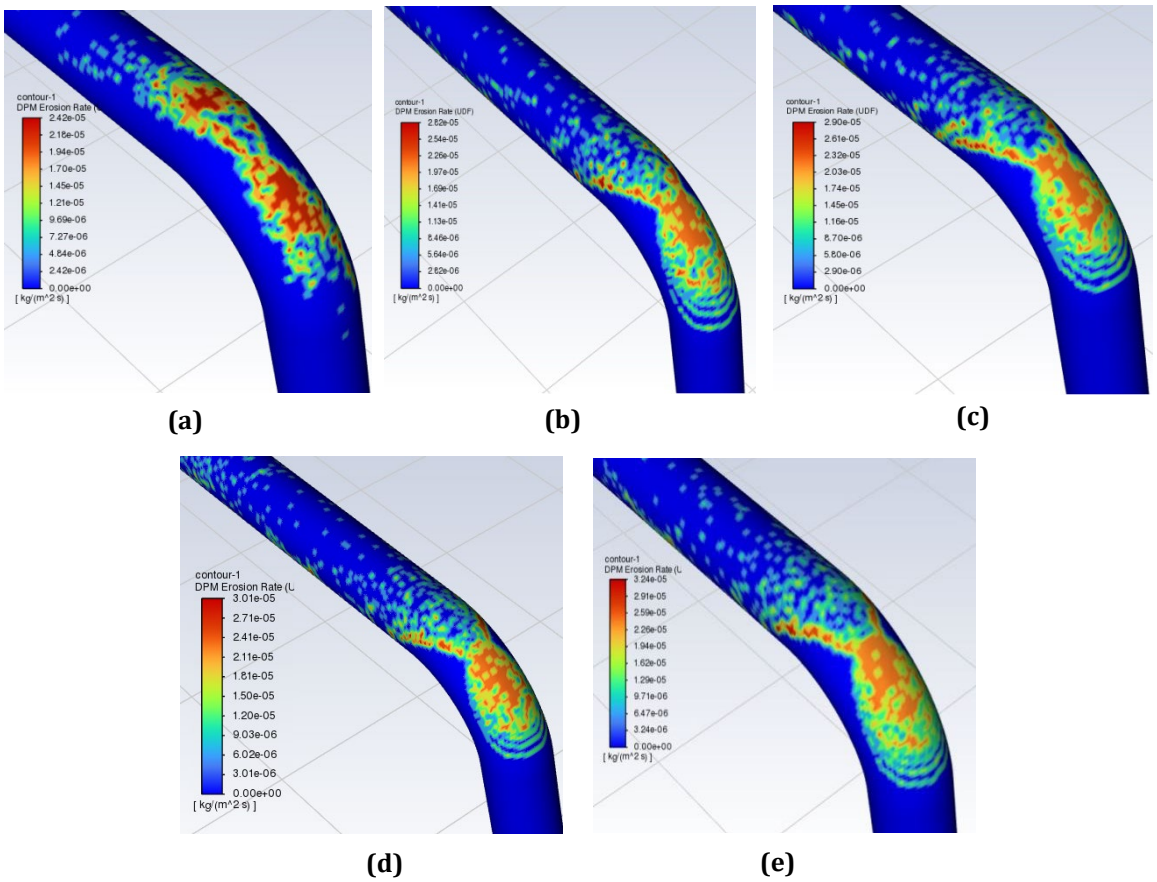

Fig. 22 *Effect of velocity on erosion rate of 25mm diameter elbow (a) 5.0m/s; (b) 12.5m/s; (c) 25m/s; (d) 37.5m/s; (e) 50m/s*

3.8.2 Straight Pipe

Straight pipeline also suffers erosion when slurries flow through it. The particles made impact on the pipe bed due to gravitational settling and turbulence in the pipeline, thereby causing erosion in the pipe bed. Pipe diameter (D) of 25mm 50mm, 75mm and 100 mm were used to investigate the erosion rate along the pipe length of 100D. Effect of velocity and mass flow rate on erosion rate was also investigated. It was observed that the erosion rate increases

Int. Journal of Integrated Engineering Vol. 16 No. 5 (2024) p. 224-249

along the pipe length. As the velocity increases, the point of dense erosion drifts far away from the inlet as shown clearly in Fig 24 (a-d). From the plot of erosion rate against velocity in Fig 23 (a) and Fig 24 (a-d), it can be concluded that the point of dense erosion drifted beyond 100D at a velocity of 50m/s, thus, the erosion on the 100D pipe spool dropped as seen in Fig 23 (a). It can be deduced that high velocity slurry flowing through a short straight pipe spool will cause little or no erosion in the pipe spool. An increase in mass flow rate reverses the trend caused by an increase in velocity. Fig. 23 (c) shows that an increase in diameter of the pipe leads to a decrease in the erosion rate. The optimal condition for minimum erosion due to coal slurry flow in straight pipeline is summarized as "large pipe diameter transports coal slurries at higher velocity and at low mass flow rate".

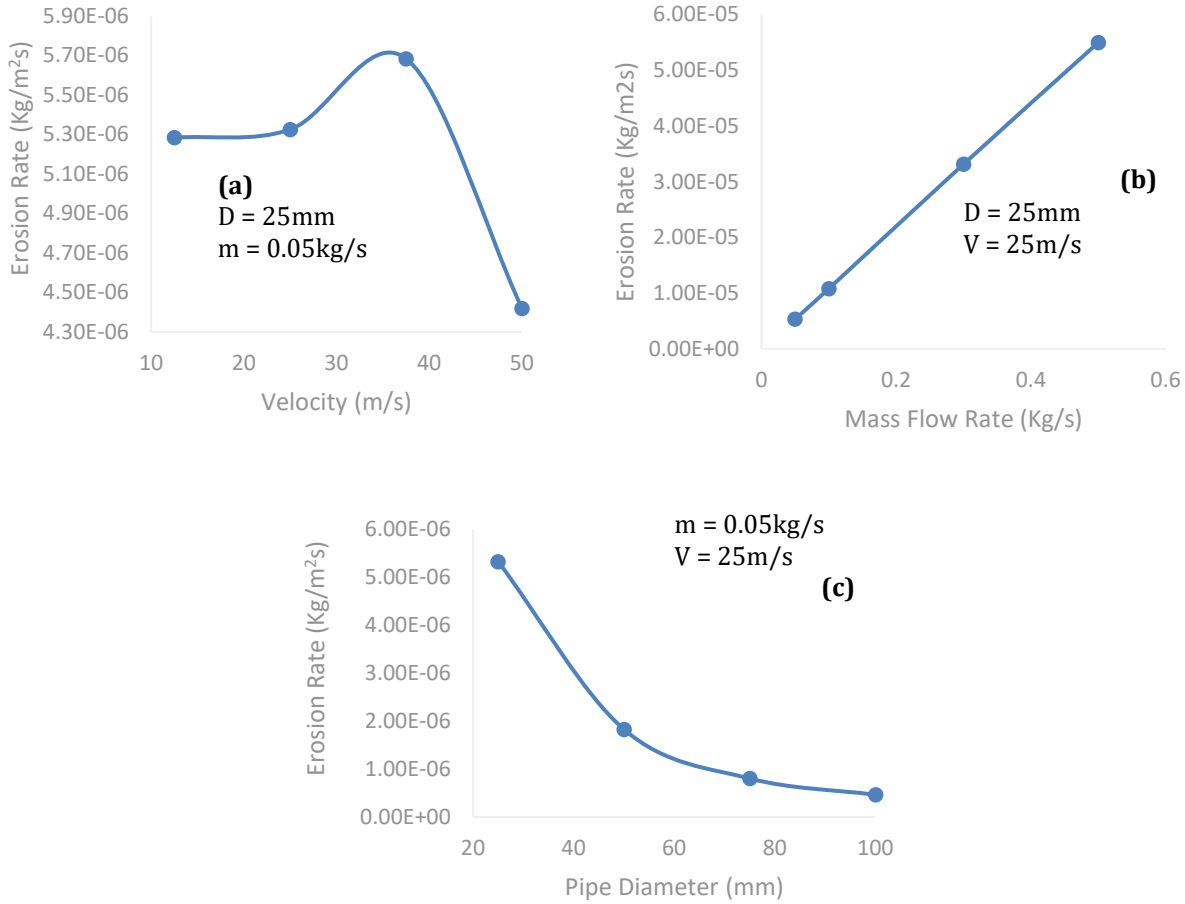

Fig. 23 *Erosion rate of 25mm diameter straight pipeline (a) effect of velocity; (b) effect of mass flow rate; (c) effect of mass pipe diameter*

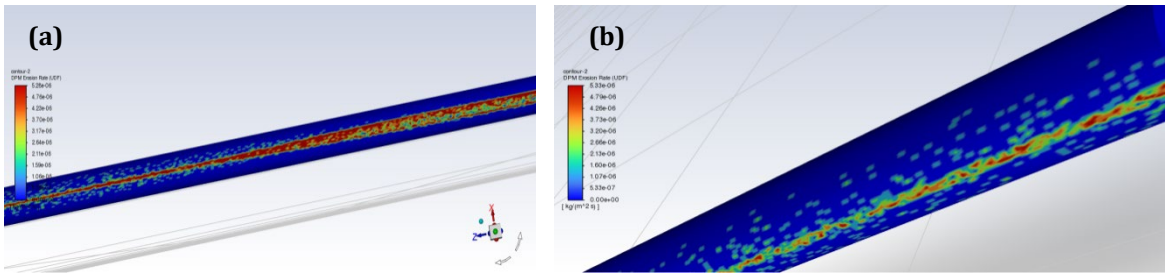

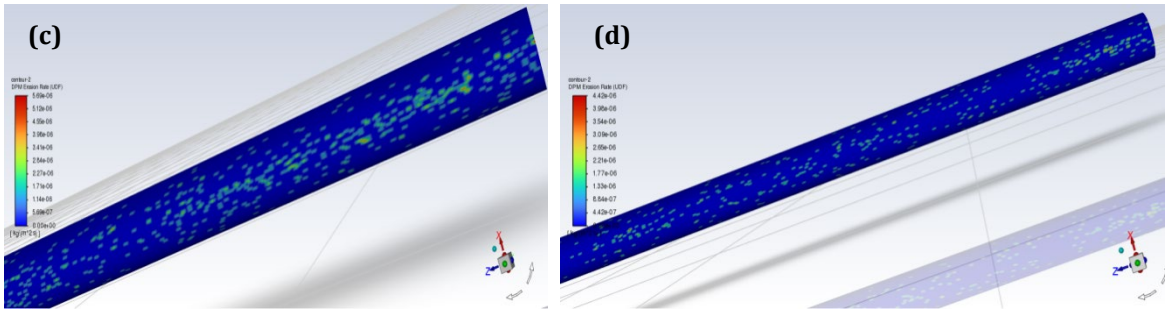

Fig. 24 *Effect of velocity on erosion rate of 25mm diameter straight pipe (a) 12.5m/s; (b) 25m/s; (c) 37.5m/s; (d) 50m/s*

4. Conclusions

A mechanistic approach inner-wall erosive wear model has been developed in this study by applying the Hertzian impact model and the impact model of Du and Wang. The model development involved determining the impact crater depth and length and computing the volume of created crater due to impact by single particle. The inner-wall mass loss rate of the target surface is determined by simple dimensional computations which involves the inclusion of the target material density and particles mass flow rate. The mechanistic approach model has been compared with experimental data and other models using ANSYS FLUENT 2021 R2 and found to have a very high level of agreement.

The following conclusions were drawn from this study:

1. It is general though validated for carbon steel in this study. Simple variation of the material constant, *k*, in the model will make it suitable for variety of target materials.
2. The results of the study show that coal-liquid slurry causes erosion in both bent and straight pipe.
3. The outcome of the simulation show that the developed model is 92% accurate when compared with the experimental values.
4. The Mechanistic model can include several parameters which are core mechanical properties of the materials that determine the level of response of its surface to erosive wear.
5. The model is responsive to material property change since many of the mechanical properties are included in it.
6. The result shows that increase in particles size (diameter) leads to increase in indentation or erosive damage.
7. The developed model incorporates many mechanical properties of both the target material and the erodent. The effect of the modulus of elasticity and the yield strength of the target material was investigated using the developed model.

The developed mechanistic model presented in this study will be useful for the accurate prediction of inner-wall erosive wear rate of pipelines conveying slurries particles in fluid, thereby reducing associated danger. The study model can be used to investigate erosion in coal slurry pipelines. It is expected that the outcome of this study will be of significant help for the strengthening of the universal application of mechanistic models for predicting erosion rate.

Conflict of Interest

Authors declare that there is no conflict of interests regarding the publication of the paper.

Human and Animal Rights

In our work, no animals or human are involved.

Informed Consent

Not applicable as no human or animal sample was involved in this study.

Acknowledgements

The authors acknowledge the financial support provided for this research by the Tertiary Education Trust Fund (TETFund), Nigeria through the Institution Based Research (IBR) Interventions 2021.

Author Contribution

The authors confirm contribution to the paper as follows: ***study conception and design****:Martins Obaseki;* ***data collection****: Martins Obaseki and Paul. T Elijah;* ***analysis and interpretation of results****: Martins Obaseki and Paul T Elijah;* ***draft manuscript preparation****: Martins Obaseki, Peter B. Alfred, Silas Oseme Okuma. All authors reviewed the results and approved the final version of the manuscript.*

References

[1] Capecelatro J. & Desjardins O. (2013). Eulerian–Lagrangian modeling of turbulent liquid–solid slurries in horizontal pipes. *International Journal of Multiphase Flow* 55 (2013) 64–79.
[2] Obaseki, M., Elijah, P.T and Alfred, P.B. (2020). Development of model to eliminate sand trapping in horizontal fluid pipelines. *Journal of King Saud University-Engineering Sciences*. https://doi.org/10.1016/j.jksues.2020.11.006.
[3] Obaseki, M., and Elijah, P., T., 2020. Dynamic modeling and prediction of wax deposition thickness in crude oil pipelines. *Journal of King Saud University-Engineering Sciences*. https://doi.org/10.1016/j.jksues.2020.05.003.
[4] Obaseki, M., Nwankwojike, B.N., & Abam, F.I., (2021). Diagnostic and Prognostics Development of a Mechanistic Model for Multiphase Flow in Oil-Gas Pipelines. *Journal of King Saud University-Engineering Sciences*. https://doi.org/10.1016/j.jksues.2020.12.010.
[5] Oka Y.I., Olmogi H., Hosokawa T. & Matsumura (1997), The impact angle dependence of erosion damage cause by solid particle impact. *Wear*, Vol. 203-204, pp573-579.
[6] Finnie I. (1958), The mechanism of erosion of ductile materials. *Proceedings of 3rd US National Congress of Applied Mechanics*. pp527-532.
[7] Bitter J.P.A. (1963a), A study of erosion phenomenon part I. *Wear*, Vol. 6, pp5-21.
[8] Bitter J.P.A. (1963b), A study of erosion phenomenon part II. *Wear,* Vol. 6, pp169-190.
[9] Neilson, J.H. & Gilchrist, A. (1968), Erosion by a stream of solid particles. *Wear* 11 (2), pp111-122.
[10] Hashish, M.1.(987), An improved model of erosion by solid particle impact. *Proceedings of the 7th International Conference on Erosion by Liquid and Solid Particle*, Cambridge, pp. 66/1- 66/9.
[11] Huang, C., Chiovelli, S., Minev, P., Luo, J. & Nandakumar, K. (2008). A comprehensive phenomenological model for erosion of materials in jet flow. *Powder Technology*. 187 (3), 273e279.
[12] McLaury, B.S. (1996). Predicting Solid Particle Erosion Resulting from Turbulent Fluctuations in Oilfield Geometries.
[13] Oka, Y.I., Okamura, K. & Yoshida, T. (2005). Practical estimation of erosion damage caused by solid particle impact: part 1: effects of impact parameters on a predictive equation. *Wear* 259 (1), 95-101
[14] Oka, Y.I. & Yoshida, T. (2005). Practical estimation of erosion damage caused by solid particle impact: part 2: mechanical properties of materials directly associated with erosion damage. *Wear* 259 (1), 102-109.
[15] Det N. V. (2007), Recommended Practice RP 0501: Erosive Wear in Piping Systems.
[16] Peng W. & Cao X. (2016), Numerical prediction of erosion distributions and solid particle trajectories in elbows for gas-solid flow. *Journal of Natural Gas Science and Engineering* 30 (2016) 455-470.
[17] Ahlert, K.R. (1994). Effects of Particle Impingement Angle and Surface Wetting on Solid Particle Erosion of AISI 1018 Steel. *Ph.D. thesis. Department of Mechanical Engineering, The University of Tulsa*.
[18] Meng H.S. & Ludema K.C. (1995), Wear model and predictive equations: their form and content. *Wear*, Vol 181-183, pp443-457.
[19] Hutchings I.M. (1981), A model for erosion of metals by spherical particles at normal incidence. *Wear*, Vol. 70, pp256.
[20] Chen, X., McLaury, B.S. & Shirazi, S.A. (2004), Numerical and experimental investigation of the relative erosion severity between plugged tee and elbow in diluted gas/solid two-phase flow. *Wear*, Vol. 261, pp715-729.
[21] Eyler, R.L. (1987), Design and Analysis of a Pneumatic Flow Loop. *M.S. thesis. West Virginia University, Morgantown, WV.*
[22] Finnie I. (1960), "Erosion of surfaces by solid particles", *Wear*, 3, 87-103.
[23] Brown G. (2006), Use of CFD to predict and reduce erosion in an industrial slurry piping system. *Fifth International Conference on CFD in the Process Industries CSIRO, Melbourne*, Australia 13-15
[24] Zhang, Y., Reuterfors, E.P., McLaury, B.S., Shirazi, S.A. & Rybicki, E.F. (2007). Comparison of computed and measured particle velocities and erosion in water and air flows. *Wear* 263 (1), 330-338.
[25] Du, Y. and Wang, S. (2009): Energy dissipation in normal elastoplastic impact between two spheres, Transactions of ASME: *Journal of Applied Mechanics*, 76, 061010-1 - 061010-8.
[26] Eyler, R.L. (1987), Design and Analysis of a Pneumatic Flow Loop. *M.S. thesis. West Virginia University, Morgantown, WV.*
[27] Bourgoyne, A.T. (1989). Experimental study of erosion in diverter systems due to sand production. In: *Proc., SPE/IADC Drilling Conference, New Orleans*, LA, SPE/IADC 18716.

[28] Bikbaev, F.A., Krasnov, V.I., Maksimenko, M.Z., Berezin, V.L., Zhilinski, I.B. & Otroshko, N.T., (1973). Main factors affecting gas abrasive wear of elbows in pneumatic conveying pipes. *Chem. Pet. Eng.* 9(1):73-75.
[29] Pyboyina, M.N. (2006). Experimental Investigation and Computational Fluid Dynamics Simulations of Erosion on Electrical Resistance Probes. *M.Sc. thesis*. Department of Mechanical Engineering, the University of Tulsa.
[30] Chi A. & Yuwei L. (2013): The model for calculating elastic modulus and poison's ratio of coal body. *The Open Fuels & Energy Science Journal*, 6:36-43.
[31] Wang C., Chen Y., He X., Yi M. &Wang Z (2019): Size effect on uniaxial compressive strength of single coal particles under different failure conditions. *Powder Technology* 345:169-181.